Journal of Mathematical Chemistry 10(1992)57–91

SELF-CONSISTENT, NONORTHOGONAL GROUP FUNCTION APPROXIMATION: AN AB INITIO APPROACH FOR MODELLING INTERACTING FRAGMENTS AND ENVIRONMENTAL EFFECTS

Ernest L. MEHLER

Department of Structural Biology, Biocenter of the University of Basel, CH-4056 Basel, Switzerland and Department of Physiology and Biophysics, Mount Sinai School of Medicine, CUNY, New York, NY 10029, USA

This paper is dedicated to Dr. Bess-Gene Holt, whose untimely death was a sad reminder to the author that our knowledge is still far from complete. Dr. Holt was a close friend whose insights and philosophy served as a strong guide to the development of the author's moral and philosophical views during his graduate student career at Iowa State University, Ames, Iowa.

Abstract

The reformulation of the single determinantal, closed shell wavefunction into an antisymmetrized product of nonorthogonal group functions (NOGF) is reviewed. It is shown that by introducing the idea of a "reciprocal" group function, i.e. a group function defined as a product of reciprocal orbitals, the resulting expressions for one- and two-electron operators are formally identical with the equations obtained using strong-orthogonal group functions. Orbital equations are given for the NOGF wavefunction which are derived by formulating a variation principle in terms of group energy functionals, where the presence of the other groups is expressed in terms of Coulomb and exchange operators in the group's Hamiltonian. To ensure that the group's orbitals do not violate the Pauli exclusion principle, a coupling or screening operator is introduced into the variational equations. The effectiveness of the coupling operator is discussed and it is demonstrated that it fully screens the group's orbitals from collapsing or distorting into forbidden regions of function space. To provide techniques for modelling and analyzing intermolecular interactions, the procedure for calculating the NGOF wavefunction can be reformulated into a series of steps which allows the components of the interaction energy, i.e. Coulomb, exchange, polarization and charge transfer, to be evaluated. This approach leads to considerable simplification and reduces the computational effort required to determine the wavefunction. The decomposition is used to analyze many-body effects in linear water chains and a model of α helical hydrogen bonding. The basis set superposition error (BSSE) in the NOGF approximation is discussed and methods for its evaluation are given, and it is shown that the BSSE is inherently less in the NOGF wavefunction than in the corresponding HF-SCF wavefunction. In the final parts of the paper, additional methods are given which further reduce computation time when both interacting fragments and their immediate environment must be considered at the quantum chemical level. These techniques are then applied to a study of the effect of environment on ion pair formation and proton transfer. The results of these studies demonstrate the remarkably strong modulating effect of molecules hydrogen bonded to the interacting pair.

1. Introduction

The single determinantal Hartree–Fock self-consistent field wavefunction (HF-SCF) has for the last thirty years been the basis for an overwhelming majority of applications and developments in quantum chemistry. The picture of molecular electronic structure it provides in the form of molecular orbital theory has been fruitful both qualitatively and quantitatively in many areas of chemistry and has strongly influenced most chemists in the way they describe the results of their investigations [1,2]. At the same time, HF-SCF theory has been the starting point of nearly all methods which seek to extend the accuracy of the wavefunction to yield a quantitative description of molecular structure, or to extend the range of applicability to larger systems.

Traditionally, the main thrust of research in the development of all-electron ab initio methods has been to extend the accurary of the HF-SCF approximation by introducing various techniques for handling electron correlation [3–6]. To extend the range of applicability to larger systems, there have been numerous improvements and refinements, both in integral evaluation and solution of the HF-SCF equations [7,8], but primary reliance has been placed on the continuing development in computational hardware and the associated enormous increase in computing speed over the last twenty years. This has allowed ab initio quantum chemistry to be applied to many systems using quite good basis sets, albeit in some cases the computational effort becomes very large. However, the recent, rapid increase in the availability of high resolution protein structures has raised new challenges for theoretical chemistry, as well as other theoretical approaches [9–11], since these systems are substantially larger and have other requirements than those ordinarily treated by ab initio quantum chemical methods.

Theoretical studies of protein chemistry, enzymatic reaction mechanisms, ligand–protein interactions and other molecular aggregations often are focussed on the interactions of a few (active) fragments (AF) embedded in an environment. To include the environmental effects, it has been suggested to divide the system into three regions [12]: I: a quantum motif which includes the interacting moiety; II: the remaining protein; and III: the bulk solvent. In this model, regions II and III are treated using classical electrostatics which is incorporated into the Hamiltonian of the quantum motif [13–16].

To provide a proper theoretical description of protein structure and function, it is essential that the noncovalent interactions be represented at least as accurately as the covalent ones. This requirement and the necessity to be able to incorporate environmental effects is most easily met by ab initio molecular orbital theory, but because of the computational demands the quantum motif usually has to be reduced to the simplest possible model, and in many cases the basis sets must also be very small. Thus all the environmental description and its modulation of the interactions of the active fragments is relegated to regions II and III. An implicit assumption of this model is that the electronic overlap between region I and regions II and III

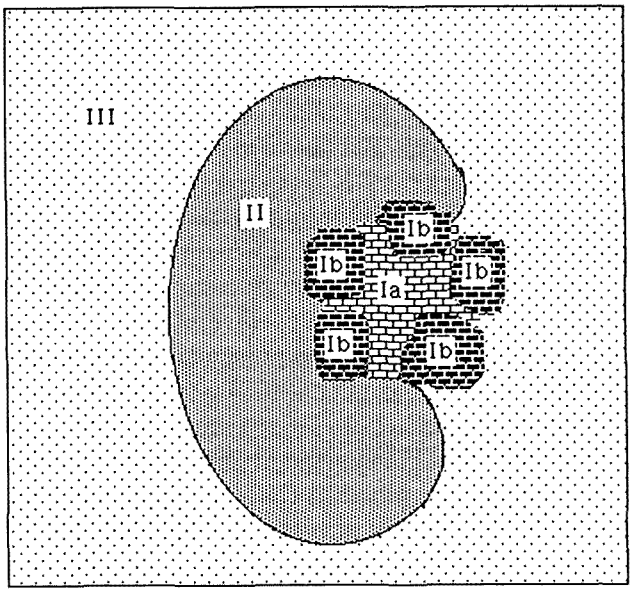

Fig. 1. Schematic representation for dividing protein and its environment into different motifs. Ia: Quantum motif containing active fragments; Ib: Quantum motif of nearest-neighbor fragments; II: Discrete electrostatic motif of remaining protein atoms; III: Continuum electrostatic motif of bulk solvent.

is essentially zero; an assumption which is not valid for those fragments which are the nearest neighbors of the AFs. A more satisfactory approach would be to also treat the nearest neighbors at the quantum chemical level which would modify the three-region model as shown in fig. 1. Here, regions II and III are as previously but region I has been split into two subregions, Ia for the active fragments and Ib for the nearest-neighbor fragments (NNF).

Naturally, the extension of region I to Ia and Ib will enlarge the quantum motif, and to be able to describe at least region Ia with reasonably accurate basis sets it is necessary to look for some simplifications of the HF-SCF approximation. Although the rate at which the number of integrals which have to be calculated formally increases with the fourth power of the number of basis functions, M, for larger aggregates the rate of increase is much slower with a lower limit of $M^2 \ln M$ [17,18]. The SCF step continues to increase, however, and eventually becomes computationally dominant so that it is reasonable to look here for further approximations.

A characteristic of the systems of interest here is that they can be divided into interacting subgroups which, because the interactions are primarily noncovalent, retain their chemical identity to a large degree. This feature suggests that a group function formulation of the single determinantal wavefunction may lead to the desired simplifications. This approach has a long history and has been used primarily

to simplify the calculation of correlated wavefunctions [19]. However, an Ansatz applicable to larger molecular aggregates was proposed some time ago [20] and it was shown that the inherent rate of increase of the method was cubic. The Ansatz is characterized by two approximations: First, the orthogonality restriction between orbitals belonging to different groups is relaxed, and second, the variational requirement of making the total energy stationary is replaced by a set of variational conditions which are used to make appropriately defined group energy functionals stationary. It was argued that in particular this latter approximation was required to achieve further economy, but it implied that the total energy obtained from the resulting wavefunction was not necessarily stationary. Nevertheless, a number of applications have shown that quantities like the interaction energy calculated with this approximation are only negligibly different from the corresponding results obtained with the standard SCF method using the same basis sets [21–24]. Because the wavefunction is constructed from a product of nonorthogonal groups, the method has been referred to as the self-consistent, nonorthogonal group function (NOGF) approximation.

Recently a new, more efficient program has been developed using the NOGF method, and a number of additional techniques were proposed to further decrease computation time [25]. These additional approximations are based on using simplified descriptions of the fragments belonging to region Ib in fig. 1, and/or removing them from the variational process. In this way, it is possible to realize further reductions in computing time and the rate at which the calculation increases with system size.

In this paper, a somewhat more general derivation of the method is given and some of its basic features and several applications are reviewed. A more detailed analysis of basis set errors in the NOGF approximation is presented and it is shown that the basis set superposition error (BSSE) in the NOGF wavefunction has a reduced distorting effect on interaction potentials and is inherently less than the BSSE in the standard SCF wavefunction constructed from the same basis. Finally, results are presented on a number of model systems which illustrate how NNFs modulate ion pair formation and proton transfers.

2. Formulation

2.1. NONORTHOGONAL GROUP WAVEFUNCTIONS, HAMILTONIAN AND ENERGY

The application of the NOGF approximation has been limited to closed shell systems in which each fragment also is assumed to be in closed shell form. Since these assumptions lead to the simplest form of the equations and most clearly exhibit the salient features of this method, only closed shell structures are considered here. The extension of the method to open shell or unrestricted cases is straightforward provided the wavefunction is expressible as a single determinant. Cases which require a linear superposition of determinants have not yet been considered.

For a system of T interacting fragments, define a fragment or group wavefunction of the form

$$\Phi_R(1,2,\ldots,2N_R) = \mathcal{A}[u_{R1}(1)u'_{R1}(2)\ldots u'_{RN_R}(2N_R) \tag{2.1}$$

for group R, where the u_{Rr} are space orbitals with α spin and the u'_{Rr} with β spin. Thus, Φ_R is a single-determinantal wavefunction made up of doubly occupied orbitals For the whole system, define an approximate wavefunction of the form

$$\Psi = \mathcal{A}' \prod_{R=1}^{T} \Phi_R(2N_{(R-1)} + 1,\ 2N_{(R-1)} + 2, \ldots, 2N_{(R)}), \tag{2.2}$$

where

$$N_{(R)} = \sum_{S=1}^{R} N_S$$

and $\mathcal{A}'$ is a partial antisymmetrizer which only exchanges electrons between groups. Orthonormality is imposed within a group, but not between groups, thus

$$\langle u_{Rr} | u_{Rr'} \rangle = \delta_{rr'} \tag{2.3a}$$

and

$$\langle u_{Rr} | u_{Ss} \rangle = S_{Rr,Ss}. \tag{2.3b}$$

It is useful to define reciprocal orbitals for the $\boldsymbol{u}$, i.e.,

$$\boldsymbol{\upsilon} = \boldsymbol{u}\mathbf{S}^{-1}, \tag{2.4}$$

where the elements of S are defined by eq. (2.3). From eq. (2.4), it is obvious that $\boldsymbol{u}^{\dagger}\boldsymbol{\upsilon} = \mathbf{I}$, that is, $\langle u_{Rr} | \upsilon_{Ss} \rangle = \delta_{Rr,Ss}$, showing that $\boldsymbol{u}$ and $\boldsymbol{\upsilon}$ are related as an orthonormal basis. There are no special orthogonality relations between the Φ_R, but now consider the "reciprocal" group defined by

$$\underline{\Phi}_R = \mathcal{A}[\upsilon_{R1}, \upsilon'_{R1} \ldots \upsilon'_{RN_R}]. \tag{2.5}$$

One then finds that

$$\int \Phi_R^*(1\ldots)\underline{\Phi}_S(1\ldots)\mathrm{d}\boldsymbol{r}_1 = 0 \qquad R \neq S. \tag{2.6}$$

Thus, Φ and $\underline{\Phi}$ are related as if they were strong-orthogonal. Norbert and McWeeny [26] have shown that the reciprocal orbital basis can be used to simplify the energy expression in valence bond theory, and eq. (2.6) suggests that this should be the case with nonorthogonal group functions as well.

The Hamiltonian can be written in the form

$$\mathcal{H} = \sum_R \mathcal{H}_R + \frac{1}{2}\sum_R g_R(S) + V_N, \tag{2.7}$$

where

$$\mathcal{H}_R = \sum_r h(Rr) + \frac{1}{2}\sum_{r \neq r'} g(Rr, Rr'), \tag{2.8a}$$

$$g_R(S) = \sum_r \sum_{S[\neq R]s} g(Rr,Ss), \tag{2.8b}$$

and $g(i,j) = 1/r_{ij}$; $h(i)$ is the one-electron part of the Hamiltonian and V_N is the total nuclear repulsion energy which can also be partitioned into one-group and two-group terms.

The expectation value of the total energy is given by

$$E = \frac{\langle \Psi | \mathcal{H} | \Psi \rangle}{\langle \Psi | \Psi \rangle}. \tag{2.9}$$

To evaluate E, it is noted that the reciprocal orbitals are defined in terms of the occupied orbitals only. Therefore, replacing the $\boldsymbol{u}$ by υ in Ψ changes the wavefunction by at most a phase factor, and by carrying out this replacement for, say, $|\Psi\rangle$ in eq. (2.9), eq. (2.6) shows that E can be evaluated as if the groups were strong-orthogonal. Inserting eqs. (2.7) and (2.8) into eq. (2.9), one obtains

$$E = \sum_R \{\langle \Phi_R | \mathcal{H}_R | \underline{\Phi}_R \rangle + \tfrac{1}{2} \langle \Phi_R \Phi_S | g_R(S) | \underline{\Phi}_R \underline{\Phi}_S \rangle + \tfrac{1}{2} V_R\}, \tag{2.10}$$

where

$$V_R = \sum_\rho \sum_{S\sigma} Z_{R\rho} Z_{S\sigma} / R_{R\rho,S\sigma} \tag{2.11}$$

and

$$g_R(S) = \sum_r \sum_{Ss} g(Rr,Ss)(1 - \mathcal{P}_{Rr,Ss}). \tag{2.12}$$

In eq. (2.11) $R\rho$ and $S\sigma$ refer to the nuclear positions in fragments R and S, respectively, and in eq. (2.12) $\mathcal{P}_{Rs,Ss}$ is a permutation operator interchanging particles between Rr and Ss. From eq. (2.10), it is seen that the total energy can be expressed as a sum of group energies, i.e.,

$$E = \sum_R E_R \tag{2.13}$$

and E_R can be further expanded to give

$$E_R = 2 \sum_r \langle u_{Rr} | h | \upsilon_{Rr} \rangle + \sum_{rSs} (2 \langle u_{Rr} u_{Ss} | \upsilon_{Rr} \upsilon_{Ss} \rangle - \langle u_{Rr} u_{Ss} | \upsilon_{Ss} \upsilon_{Rr} \rangle) + \tfrac{1}{2} V_R. \tag{2.14}$$

In the above formulation, the total energy is obtained as an exact sum of group energy quantities [27]. An alternative form is obtained by considering the electrons of a given fragment moving in the average field generated by the electrons and nuclei of the other fragments [28,29]. For the group R, one writes

$$E'_R = \langle \Phi_R | \mathcal{H}_R | \underline{\Phi}_R \rangle + \sum_{S(\neq R)} \langle \Phi_R \Phi_S | g_R(S) | \underline{\Phi}_R \underline{\Phi}_S \rangle + V'_R, \tag{2.15}$$

where

$$V'_R = \tfrac{1}{2}\sum_{\rho\rho'} Z_{R\rho}Z_{R\rho'} / R_{R\rho,R\rho'} + \sum_{\rho S(\neq R)\sigma} Z_{R\rho}Z_{S\sigma} / R_{R\rho,S\sigma}$$

$$= \tfrac{1}{2} V_{RR} + V_{RS}, \tag{2.16}$$

and E is then given by

$$E = \sum_R E'_R - \tfrac{1}{2}\sum_{S(\neq R)} \{\langle \Phi_R\Phi_S | g_R(S) | \underline{\Phi}_R\underline{\Phi}_S\rangle + V_{RS}\}. \tag{2.17}$$

As a result of the strong orthogonality-like relationship in eq. (2.6), the energy formulas given in eqs. (2.10) and (2.17) are structurally identical with those obtained for strong-orthogonal groups [28,29]. Moreover, when E_R is expanded in orbital form, eq. (2.14), the resulting expression for the total energy is formally identical with the standard expression obtained for the single-determinantal wavefunction of a closed shell system using orthonormal orbitals. Since the system's density matrix is given by

$$\rho = 2\sum_{Ss} |u_{Ss}\rangle\langle v_{Ss}|, \tag{2.18}$$

the only extra computation required to evaluate E is the calculation and inversion of S, which is trivial.

2.2. GROUP ENERGIES AND VARIATIONAL PROCEDURES

The wave function defined in eq. (2.2) is, of course, just the closed shell Hartree–Fock wavefunction written in a modified form. The fact that nonorthogonal functions have been used does not make it more or less general. Although it is possible to proceed by making E stationary, this would not yield anything new since the resulting orbital equations just would be the HF-SCF equations in a more complicated form. This approach has been studied by various authors [30–37] to obtain orbitals in a specialized form, but in most cases it has proven to be more practical to solve the canonical HF-SCF equations and then transform the orbitals to the desired form. It is clear, therefore, that to obtain simpler orbital equations the requirement that E be stationary has to be relaxed which can be accomplished by modifying the standard variational procedure.

The relaxation of the intergroup orthogonality constraints allows each group to be considered independently with its electrons moving in an average field generated by the electrons of the other groups. This consideration suggests that an appropriate group energy functional should be similar in form to E'_R given in eq. (2.15). However, since we are considering the groups as independent entities, the energy functional is defined by

$$\mathcal{E}^R = \langle \Phi_R | \mathcal{H}^R | \Phi_R \rangle / \langle \Phi_R | \Phi_R \rangle, \tag{2.19}$$

where $\mathcal{H}^R$ is an effective Hamiltonian defined by

$$\mathcal{H}^R = \sum_i h^R(i)_{\text{eff}} + \sum_{i<j} g(i,j) \tag{2.20}$$

and

$$h^R(1)_{\text{eff}} = h(1) + \sum_{S(\neq R)s} [2\mathcal{J}_{Ss}(1) - \mathcal{K}_{Ss}(1)], \tag{2.21}$$

where $\mathcal{J}$ and $\mathcal{K}$ are the Coulomb and exchange operators, respectively [20], Both the Coulomb and exchange operators are required in h^R_{eff} since intergroup orbital overlaps are not zero. From eqs. (2.1), (2.3a), (2.20) and (2.21), one obtains

$$\mathcal{E}^R = 2\sum_r \langle u_{Rr} | h^R_{\text{eff}} | u_{Rr} \rangle + \sum_{rr'} [\langle u_{Rr} | 2\mathcal{J}_{Rr'} - \mathcal{K}_{Rr'} | u_{Rr} \rangle]. \tag{2.22}$$

In the case of strongly orthogonal group functions, $\mathcal{E}^R$ and E'_R would be identical and the total energy would be given by eq. (2.17) [28]. However, here $\mathcal{E}^R$ is expressed in terms of the local group density matrices

$$\rho^R = 2\sum_r |u_{Rr}\rangle\langle u_{Rr}|, \tag{2.23}$$

and since

$$D\rho = \rho - \sum_S \rho^S \neq 0, \tag{2.24}$$

it is usually not possible to express the total energy in terms of the $\mathcal{E}^R$. Moreover, making the $\mathcal{E}^R$ stationary no longer guarantees that E is stationary except when the groups have been made strong orthogonal by, say, construction, symmetry, etc. Since in the latter case stationary $\mathcal{E}^R$ would yield the HF-SCF solution, giving a well-defined basis of comparison, it seems reasonable to obtain the orbital equations from the variational condition $\delta \mathcal{E}^R = 0$ for $R = 1, 2, \ldots, T$.

The general problem of making a functional stationary in a restricted subspace has been discussed elsewhere [38,39], and in the context of strongly orthogonal group functions by McWeeny [28,29]. In the present case, it is required to make $\mathcal{E}^R$ stationary with respect to the $|u_{Rr}\rangle$, which in general will only span a part of Hilbert space. Moreover, if the groups are strong-orthogonal the wavefunction will automatically satisfy the Pauli principle, provided that the groups are constrained to remain strong-orthogonal when optimized. Here the groups are not strong-orthogonal, and their variation has to be constrained in such a way that the Pauli principle is not violated between electrons belonging to different groups. This can be accomplished by requiring the intergroup orbital overlaps $\langle u_{Rr} | u_{Ss} \rangle$ to remain constant while the orbitals of the Rth group are varied. In addition, it is required that intragroup

orthonormality be conserved. The complete variational problem may be expressed as follows:

$$\delta \mathcal{E}^R = 0, \tag{2.25a}$$

$$\delta\langle u_{Rr} | u_{Rr'}\rangle = 0 \tag{2.25b}$$

and

$$\delta[\langle u_{Rr} | u_{Ss}\rangle + \langle u_{Ss} | u_{Rr}\rangle] = 0 \quad \{|u_{Ss}\rangle, (S \neq R), \text{ constant}\}. \tag{2.25c}$$

Both sets of constraints can be incorporated into the variational problem by the usual method of Lagrangian multipliers. One obtains

$$\mathcal{F}^R |u_{Rr}\rangle = \sum_{Ss} \lambda_{Ss,Rr} |u_{Ss}\rangle \qquad R = 1,2,\ldots,T, \tag{2.26}$$

where

$$\mathcal{F}^R = h^R_{\text{eff}} + \sum_r 2\mathcal{J}_{Rr} - \mathcal{K}_{Rr}. \tag{2.27}$$

On multiplying both sides of eq. (2.26) by $\langle v_{Ss}|$, one obtains

$$\lambda_{Ss,Rr} = \langle v_{Ss} | \mathcal{F}^R | u_{Rr}\rangle, \tag{2.28a}$$

but for group S, one gets

$$\lambda_{Rr,Ss} = \langle v_{Rr} | \mathcal{F}^S | u_{Ss}\rangle. \tag{2.28b}$$

If the orbitals had been chosen orthonormal, and therefore the groups strong-orthogonal, one would have $\mathbf{S} = \mathbf{I}$ and thus $|v_{Rr}\rangle = |u_{Rr}\rangle$, from which it obviously follows that

$$\lambda_{Rr,Ss} = \lambda_{Ss,Rr}, \tag{2.29}$$

showing that eqs. (2.26) would yield the standard HF solution. However, for the nonorthogonal case, eq. (2.29) does not hold so that it is not possible to find an orthogonal transformation which makes all the off-diagonal elements of λ vanish simultaneously. Alternatively, it is possible to express λ in terms of a coupling operator [31] by multiplying both sides of eq. (2.28a) by $|u_{Ss}\rangle$ and then summing over all groups and orbitals to give

$$\sum_{Ss} [|u_{Ss}\rangle\langle v_{Ss}| \mathcal{F}^R |]|u_{Rr}\rangle = \sum_{Ss} \lambda_{Ss,Rr} |u_{Ss}\rangle. \tag{2.30}$$

The term $\sum |u_{Ss}\rangle\langle v_{Ss}|$ is a general projection operator [38] and the term in square brackets is a coupling or screening operator. Substituting the l.h.s. of eq. (2.30) and its Hermitian extension into eq. (2.26), and at the same time adding the term $\lambda_{Rr,Rr}|u_{Rr}\rangle$ $(\equiv \varepsilon_{Rr}|u_{Rr}\rangle)$ to both sides of eq. (2.26), one obtains

$$\mathcal{G}^R|u_{Rr}\rangle = \varepsilon_{Rr}|u_{Rr}\rangle \quad R = 1,2,\ldots,T, \tag{2.31}$$

where

$$\mathcal{G}^R = 2\mathcal{F}^R - \sum_{Ss}(|u_{Ss}\rangle\langle v_{Ss}|\,\mathcal{F}^R + \mathcal{F}^R|v_{Ss}\rangle\langle u_{Ss}|) + \sum_{r'}|u_{Rr'}\rangle\langle v_{Rr'}|\,\mathcal{F}^R|u_{Rr'}\rangle\langle u_{Rr'}|. \tag{2.32}$$

The variational procedure developed here has reduced the standard Fock matrix to a block-diagonal form where the dimensionality of each block is dependent on N_R. The form of the screening operator introduced in eq. (2.32), i.e., $\rho\mathcal{F} + \mathcal{F}\rho$, is essentially that first proposed by Gilbert [32,33], whereas Adams [30,31] used a different form, $\rho\mathcal{F}\rho$, to derive his localized orbital equations. Both these operators screen the group from the environment, but it is clear that the latter form is more complex than the former. In particular, from eq. (2.18) it is easy to show that construction of the elements of $\rho\mathcal{F} + \mathcal{F}\rho$ requires at most two-electron integrals which couple three groups, whereas $\rho\mathcal{F}\rho$ also requires two-electron integrals coupling four groups. Both of these operators provide full screening of the group Fock operator $\mathcal{F}^R$. Other approaches which have been used to simplify the Adams–Gilbert equations result in a reduced screening, e.g., $\rho^R\mathcal{F}^R\rho^R$, but these are generally not sufficient [41,42].

2.3. BASIS EXPANSIONS AND PROGRAM STRUCTURE

To solve the NOGF equations, the orbitals are expanded in a basis

$$u_{Rr} = \sum_{\rho=1}^{M_R}\chi_{R\rho}C_{R\rho,Rr}, \tag{2.33}$$

where M_R is the number of basis functions used in the expansion of the orbitals of group R. Due to the relaxation of the orthogonality constraints between groups, $M_R \leq M$, where M is the total number of basis functions. The formulation of the NOGF approximation allows the basis functions to be distributed between the groups in an arbitrary way, although some distributions will be chemically more meaningful than others.

The reciprocal orbitals are defined by

$$v_{Ss} = \sum_{S\sigma=1}^{M}\chi_{S\sigma}d_{S\sigma,Ss}, \tag{2.34}$$

where

$$d_{S\sigma,Rr} = \sum_{s}C_{S\sigma,Ss}(\mathbf{S}^{-1})_{Ss,Rr}. \tag{2.35}$$

With these definitions, the groups' and system's density matrices are written as

$$\rho^R = 2\mathbf{C}^R\mathbf{C}^{R\dagger} \tag{2.36}$$

and

$$\rho = 2\mathbf{C}\,\mathbf{d}^{\dagger}. \tag{2.37}$$

$\mathbf{C}^R$ is a square $M_R \times M_R$ matrix of the group's expansion coefficients, but both $\mathbf{C}$ and $\mathbf{d}$ are square $M \times M$ matrices where the structure of $\mathbf{C}$ is block diagonal [20]. Using eqs. (2.36) and (2.37), the NOGF equations can be developed in matrix form. This has recently been done elsewhere and the reader is referred there for the details [25].

The orbital equations (2.31) define two levels of iteration, namely an intragroup level where a given group is brought to self-consistency in the fixed field of the other groups, and an intergroup level which brings the whole system to self-consistency. Examination of the structure of $\mathcal{G}^R$ shows that the electron-interaction integrals which appear in the equations can be classed in four types $(RR|RR)$, $(RS|RR)$, $(RR|AA)$, and $(RS|AA)$ [25]. Since only integrals coupling up to three groups are required for solving eqs. (2.31), the rate of increase of computational effort for solving the SCF equations reduces from a quartic to a cubic dependence. During an intragroup iteration only the first two types need to be updated at each iteration step, whereas for intergroup iterations all four types have to be updated. Considerable economy can therefore be achieved by constructing the computational algorithm to allow for both levels of iteration.

In constructing the coupling operator, it was necessry to use the complete projection operator, i.e. ρ, which then required the use of a level shift operator to be able to recover the orbital eigenvalues. However, as noted above, λ is not Hermitian and there is no assurance that the canonical orbitals are obtained. To do so would in general require a complex transformation to diagonalize λ^R. Inspection of the off-diagonal elements of λ^R shows, however, that the non-Hermiticity is not very great and in order to restrict the program to real arithmetic, only the Hermitian part of λ^R is diagonalized. It should also be noted that the validity of Koopman's theorem [43] for the NGOF wavefunction has not been established.

2.4. EFFICACY OF THE COUPLING OPERATOR

The capacity of the coupling operator to screen the group from the environment is crucial to obtain wavefunctions with a proper structure. In addition to preventing variational collapse or distortion by keeping a group's occupied orbitals from moving into forbidden regions of function space, the coupling operator will tend to localize the group's orbitals. As will be seen below, this localization permits a decomposition of intermolecular interaction quantities to be developed which exploits the group product structure of the wavefunction, and allows the introduction of a number of additional approximations which help to reduce the computation for larger aggregates.

The effectiveness of the coupling operator can be better appreciated by a simple example. Calculations were performed on the linear HF dimer [44], and Huzinaga's (9s, 5p) basis was used for fluorine and his (4s) basis for hydrogen [45]. This primitive atomic basis was contracted to a double zeta orbital basis using Dunning's contraction coefficients [46]. The experimental HF separation of 1.03 Å was used [47]. Calculations were carried out at three intermolecular distances to determine the minimum and interaction energy.

Table 1

Group structure for linear $F_1-H_1-F_2-H_2$.

Group	Basis
1	F_1: 1s, 2s
2	F_2: 1s, 2s
3a	F_1: 3s, 4s
3b	F_1: 1z, 2z; H_1: 1s, 2s; F_2: 3s, 4s
3c	F_2: 1z, 2z; H_2: 1s, 2s
4	F_1: 1x, 2x; F_2: 1x, 2x
5	F_1: 1y, 2y; F_2: 1y, 2y

Table 1 gives the assignments of the orbitals to the groups. The inner shells of F_1 and F_2 are assigned to groups 1 and 2, respectively. Group 3 comprises the σ part of the valence shell, while groups 4 and 5 are occupied by the π electrons. Due to symmetry, groups 4 and 5 are strong-orthogonal to each other and to the σ groups, and do not have to be included in the coupling operator. Wavefunctions with three different group product structures were considered:

$$\Psi_A = \mathcal{A}'[\Phi_{123}\Phi_4\Phi_5],$$

$$\Psi_B = \mathcal{A}'[\Phi_1\Phi_2\Phi_3\Phi_4\Phi_5], \tag{2.38}$$

$$\Psi_C = \mathcal{A}'[\Phi_1\Phi_2\Phi_{3a}\Phi_{3b}\Phi_{3c}\Phi_4\Phi_5].$$

Ψ_A is just the standard HF-SCF wavefunction, while in Ψ_B the F 1s cores have been separated from the valence shell electrons. Ψ_C is similar to Ψ_B, but the valence shell has been further split as given in table 1. The additional decomposition of the valence shell in Ψ_C further localizes the H-bonding region of the dimer.

The results of the calculations are summarized in table 2, where a number of properties are compared. Examination of the orbital energies of Ψ_B and Ψ_C shows that they are all close to the values obtained from Ψ_A. Especially for $\pi 1,2$ the differences are only about 0.25 eV. It is also seen that the errors in Ψ_C's orbital energies are somewhat larger than those from Ψ_B. Comparison of the dipole moment,

Table 2

Comparison of properties from different wavefunctions and couplings.

$\Psi^{a)}$	A		B	$B'^{b)}$		C	$C'^{c)}$
$\Phi_{R,r}$	$-\varepsilon$	$\Phi_{R,r}$	$-\varepsilon$	$-\varepsilon$	$\Phi_{R,r}$	$-\varepsilon$	$-\varepsilon$
$\sigma 1,1$	26.3419	$\sigma 2,1$	26.3323	26.1686	$\sigma 2,1$	26.3200	26.3089
$\sigma 1,2$	26.2504	$\sigma 1,1$	26.2416	26.1966	$\sigma 1,1$	26.2581	26.7569
$\sigma 1,3$	1.6556	$\sigma 3,1$	1.6351	5.8797	$\sigma 3b,1$	1.5727	2.1357
$\sigma 1,4$	1.5653	$\sigma 3,2$	1.5457	5.7980	$\sigma 3a,1$	1.5049	1.8207
$\sigma 1,5$	0.8309	$\sigma 3,3$	0.8215	0.7381	$\sigma 3c,1$	0.8296	0.7926
$\sigma 1,6$	0.7081	$\sigma 3,4$	0.6981	0.6697	$\sigma 3b,2$	0.7608	1.5982
$\pi 1,1$	0.6995	$\pi 4,1$	0.6902	0.5581	$\pi 4,1$	0.6759	0.9677
$\pi 1,2$	0.6086	$\pi 5,1$	0.6000	0.5314	$\pi 5,1$	0.6129	0.6426
$-E$	200.0427		199.9006	195.8807		199.8743	198.3292
μ	1.9836		1.9848	−0.3706		2.0128	0.4315
R_e	5.44		5.44			5.48	
$-\Delta E$	6.15		6.52			5.41	

[a)] Group product structure, see eq. (2.38) in text; properties in atomic units except ΔE in kcal/mole.
[b)] Structure as B, but screening operator excluded.
[c)] Structure as C, but screening partially excluded (see text).

equilibrium separation and interaction energy obtained with Ψ_B and Ψ_C shows that these quantities are in good agreement with the HF-SCF results. It appears, therefore, that the screening provided by the coupling operator is adequate to prevent any type of variational distortion in the group wavefunctions Ψ_B and Ψ_C.

To see this more clearly, the wavefunctions $\Psi_{B'}$ and $\Psi_{C'}$ have the same structure as Ψ_B and Ψ_C, respectively, but the coupling between one or more groups has been turned off. In $\Psi_{B'}$, the coupling operator has been completely excluded and it is clear from the orbital energy values of $\sigma 3,1$ and $\sigma 3,2$ that they are trying to mimic the cores of F_1 and F_2. The other orbitals are also distorted, the total energy is much too high and the dipole moment is completely incorrect. Comparison of $\Psi_{B'}$ with Ψ_B provides a dramatic illustration of the necessity of screening in this type of formulation. Although the distortions seen in $\Psi_{C'}$ are smaller than in $\Psi_{B'}$, they are still considerable. Here, only the coupling between groups 3b and 3a has been eliminated when 3b was being varied. 3b describes the hydrogen bonding interaction and it is clear that both $\varepsilon_{3b,1}$ and $\varepsilon_{3b,2}$ are much too low. Other valence shell orbital energies also show large errors. Thus, the wavefunction is again distorted as indicated by the values of the total energy and dipole moment. The latter, although better than the result calculated from $\Psi_{C'}$ is still far away from the HF-SCF value. It is clear from these latter results that not only variational collapse into the inner shell leads to problems, but that any kind of variational distortion yields wavefunctions which are seriously in error.

3. Modelling intermolecular interactions

A group product structure of the wavefunction is particularly suitable for the study of noncovalent interactions because in these types of systems the interacting fragments are not too strongly perturbed from the structures of the isolated subsystems and therefore retain their chemical identity. It is then also straightforward to set up the structure of the wavefunction since the groups are most naturally based on all wavefunctions of the corresponding isolated fragments. The group operator $\mathcal{G}^R$ (eq. (2.32)) does not contain any explicit localization terms, thus the degree of localization of any group's orbitals is controlled by the definition of the basis expansion (eq. (2.33)), which only has to span a part of basis space, and the coupling operator. In the previous section, it has been shown that the latter is sufficient for keeping the groups localized in their own proper subspaces. The relaxation of the orthogonality constraints provides additional flexibility for constructing the NOGF wavefunction since the orbitals no longer have to span the entire space. This added degree of freedom allows a natural decomposition of the interaction energy to be derived, and makes possible the implementation of further approximations which result in additional computational economy with only a small or negligible loss in the quality of the wavefunction.

3.1. DECOMPOSITION OF THE INTERACTION ENERGY

We now associate the T group functions with an aggregate of T noncovalently interacting fragments. For each isolated subsystem, the single determinantal wavefunction Φ_R^0 has been determined with energy $\mathcal{E}_0^R = \langle \Phi_R^0 | \mathcal{H}_0^R | \Phi_R^0 \rangle$, where $\mathcal{H}_0^R$ is the Hamiltonian of the isolated system. The orbitals are given by

$$u_{Rr}^0 = \sum_{\rho=1}^{M_R} \chi_{R\rho} C_{R\rho,Rr}^0 . \tag{3.1}$$

Now construct the wavefunction

$$\Psi_1 = \mathcal{A}'[\Phi_1^0 \Phi_2^0 \ldots \Phi_T^0]. \tag{3.2}$$

Since Ψ_1 is constructed from the unperturbed orbitals of the isolated subsystems, the quantity

$$\Delta E_{C+EX} = E_1 - \sum_{S=1}^{T} \mathcal{E}_0^S \tag{3.3}$$

yields the Coulomb and exchange contributions to the interaction energy. In eq. (3.3), E_1 is the total energy calculated from Ψ_1. From the Hartree group product, i.e., $\Psi_0 = [\Phi_1^0 \Phi_2^0 \ldots \Phi_T^0]$, one can calculate the Coulombic contribution explicitly. It is easily shown [21] that both electrostatic and exchange contributions calculated from

the NOGF wavefunction are exactly identical with Morokuma's definition of this quantity [48]. The NOGF orbital equations (2.31) are now solved for the unperturbed orbitals of Ψ_1 to obtain

$$\Psi_2 = \mathcal{A}'[\Phi_1\Phi_2 \ldots \Phi_T]. \tag{3.4}$$

The group orbitals of Ψ_2 are still expanded in the basis of the isolated subsystem, and have the form

$$u_{Rr} = \sum_{r'}^{\text{occ}} u^0_{Rr'}\, a_{Rr',Rr} + \sum_{r'}^{\text{vir}} u^0_{Rr'}\, b_{Rr',Rr}\,. \tag{3.5}$$

Therefore, Ψ_2 also includes the polarization of each group's charge distribution induced by the other groups, and the polarization energy is evaluated from

$$\Delta E_{\text{Pol}} = E_2 - E_1\,. \tag{3.6}$$

In the final step of this decomposition, the orbitals are expanded in the form

$$u_i = \sum_{Rr'}^{\text{occ}} u^0_{Rr'}\, a_{Rr',i} + \sum_{Rr'}^{\text{vir}} u^0_{Rr'}\, b_{Rr',i}\,, \tag{3.7}$$

and the standard HF-SCF wavefunction

$$\Psi_3 = \Phi_{1,2,\ldots,T} \tag{3.8}$$

is formed which now also includes the charge transfer effects. The charge transfer (CT) contribution is obtained from

$$\Delta E_{\text{CT}} = E_3 - E_2\,, \tag{3.9}$$

and the total interaction energy is given by

$$\Delta E = \Delta E_{\text{C+EX}} + \Delta E_{\text{Pol}} + \Delta E_{\text{CT}} = E_3 - \sum \mathcal{E}_0^S\,. \tag{3.10}$$

The decomposition of the NOGF wavefunction is similar but not identical with the decomposition of the HF-SCF wavefunction developed by Morokuma [48] and others [49,50]. The difference is due to the fact that with the NOGF wavefunction the induction effects can also be obtained from a fully antisymmetrized wavefunction. The earlier decompositions of the HF-SCF wavefunction used a Hartree product for calculating the polarization [51] and then passed directly to the final wavefunction (eq. (3.8)), which yielded a quantity comprising the charge transfer contribution and all other higher-order terms. By an appropriate analysis of the Fock matrix, Morokuma succeeded in decomposing this last term into three terms, i.e., charge transfer, exchange-polarization and mixing [48].

It was shown by a perturbation analysis of the orbitals of Ψ_2 [21] that the first-order contribution (Coulombic and exchange) obtained from the NOGF wavefunction is identical with the Coulomb and exchange energy obtained from the HF-SCF wavefunction. The second-order term, however, is different. Besides the polarization energy obtained from the Hartree product [51], the exchange-polarization (expl) contribution is also included. This comes about because Ψ_2 is fully antisymmetrized. In addition, the screening operator also contributes a term which is repulsive and partially compensates the expl contribution. This latter term is an interaction between the virtual orbitals of the Rth group and the occupied orbitals of the other groups and is therefore part of the polarization interaction. It vanishes if the orbitals become orthogonal.

Table 3

Comparison of NOGF and HF-SCF energy decomposition

	$(H_2O)_2$[a]		$(HF)_2$[a]	
Interaction[b]	NOGF	HF-SCF[c]	NOGF	HF-SCF[d]
C + EX	− 4.8	− 4.8	− 4.1	− 4.1
Pol	− 0.7	− 0.5	− 0.5	− 0.3
CT	− 2.2	− 2.1	− 2.9	− 2.9
EXPL + MIX		− 0.3		− 0.2
ΔE	− 7.7	− 7.7	− 7.5	− 7.5

[a] R(O−O) = 2.98 Å; R(F−F) = 2.79 Å, see ref. [21]; energy in kcal/mole.
[b] C: electrostatic; EX: exchange; Pol: polarization; CT: charge transfer; EXPL: exchange-polarization, ref. [48]; MIX: mixing, ref. [48].
[c] Ref. [48].
[d] Ref. [54].

Table 3 summarizes the results of applying the NOGF decomposition to the water and HF dimers [21] and compares it with the results obtained from the HF-SCF wavefunctions using Morokuma's extended approach [48]; 4-31G bases [52] and identical geometries were used for the calculations. The result of the differences in the definition of the polarization wavefunction is that the polarization contribution obtained from the NOGF decomposition is lower than the HF-SCF value. However, the NOGF charge transfer is practically identical with the value obtained from the HF-SCF calculation using Morokuma's extended definition [48]. In the NOGF approximation, a natural decomposition is obtained, where each intermediate component is calculated from a properly antisymmetrized wavefunction. Moreover, all the polarization terms are accounted for by Ψ_2 so that ΔE_{CT} contains only charge transfer and the very small remaining higher-order mixing terms.

3.2. CHARGE TRANSFER IN THE NOGF APPROXIMATION

Since the decomposition scheme given above ends with the standard HF-SCF wavefunction, all interactions describable with a single determinantal wavefunction are accounted for. However, for application to large molecular aggregates this is not particularly useful since to complete the analysis the HF-SCF wavefunction is required. Of course, one could simply stop with the polarization wavefunction Ψ_2 and neglect the charge transfer contribution. However, this is not really acceptable since many applications have shown that CT makes an important contribution to the interaction energy [21,53,54] as well as to other properties.

A way to proceed is suggested from the fact that CT is a fairly rapidly decreasing function of interfragment separation, and involves primarily groups with nonzero overlap. As discussed by Morokuma [48], charge transfer can be interpreted as a delocalization which is realized by mixing the occupied space of one fragment with the virtual space of another. The group orbitals defined by eq. (3.5) cannot do this since they only include the intragroup occupied and virtual spaces. Thus, in order to give a group access to the virtual space of another group, its orbital expansions need to be extended to include at least part of the basis space of any group with which CT can occur. These orbitals are therefore expanded in the form

$$u^{e}_{Rr} = \sum_{\rho=1}^{M_R} \chi_{R\rho} C_{R\rho,Rr} + \sum_{S(\neq R)\sigma} \chi_{S\sigma} C_{S\sigma,Rr}\,, \tag{3.11}$$

where the superscript "e" denotes that the orbital's expansion has been extended. In eq. (3.11), the first term is as above and just includes the entire basis space of the fragment R, but the second sum includes basis functions from other groups. Naturally, it will be advantageous to keep the second sum as short as possible to save computing time.

For hydrogen bonding it turns out that the situation is especially simple, since it has been found that a complete accounting of CT effects is obtained by including the H-bonding proton's atomic basis in the proton acceptor's (PA) as well as in the proton donor's (PD) basis. Thus, only the PA's orbitals have to be extended. The NOGF wavefunction for an H-bonded dimer is $\Psi = \mathcal{A}'[\Phi^{e}_{PA}\Phi_{PD}]$ and a comparison of the CT contribution for several dimers [21] is given in the first two columns of table 4. The calculated difference in the CT energy obtained from eq. (3.9) and using extended orbitals in the PA's group function is about 0.7 kcal/mole except for HNC-HF, where it is substantially larger. However, the CT term is always contaminated with a BSSE, and its value will not be the same in the two types of wavefunction used in the calculations listed in table 4.

3.3. BSSE IN THE NOGF APPROXIMATION

In the supermolecule approach to studying molecular interactions, the BSSE is a well-known artifact arising from the requirement that finite bases have to be

Table 4

Comparison of CT energy contributions of H-bonded dimers.

Dimer	E_{CT}[a]	E'_{CT}[a]	Δ[b]	Corr E_{CT}[c]	Corr E'_{CT}[c]	Δ[b]
$(H_2O)_2$	2.2	1.5	0.7	0.8	0.7	0.1
$(HF)_2$	2.9	2.1	0.8	1.0	1.0	0.0
H_2O-HF	2.5	1.9	0.6	1.3	1.4	−0.1
HCN−HF	1.9	1.1	0.8	0.7	0.7	0.0
HNC−HF	4.1	2.3	1.8	1.3	1.0	0.3

[a] Energy in kcal/mole; unprimed quantity from eq. (3.9); primed quantity uses extended group orbitals, eq. (3.11).
[b] $\Delta = E_{CT} - E'_{CT}$.
[c] Corrected for BSSE.

used for actual calculations [55]. Several proposals have been made for calculating the "true" BSSE [56,57], but because of its computational simplicity, the technique originally proposed by Boys and Bernardi [58] remains the most commonly used approach. Moreover, recent studies seem to indicate that it is the most reliable correction available [59,60]. In this method, the correction is calculated for each isolated fragment from the difference

$$\Delta E_{BSSE} = \mathcal{E}_0(\text{fragment in supermolecule basis}) - \mathcal{E}_0. \tag{3.12a}$$

The correction is calculated for each fragment and then summed to give the total BSSE contribution.

The counterpoise technique can also be used to correct the interaction energy calculated from the NOGF wavefunction, but the method has to be slightly modified. The BSSE will only be present in groups which use extended orbitals and only those basis functions are included which actually appear in the group's orbital expansion. In the H-bonding case, therefore, only PAs have to be considered [21]. The correction is defined by

$$\Delta E'_{BSSE} = \mathcal{E}_0(\text{fragment + proton's basis}) - \mathcal{E}_0. \tag{3.12b}$$

Comparing eq. (3.12b) with eq. (3.12a) shows that in the NOGF approximation, the correction can never be greater than when using the standard wavefunction. The BSSE correction has been applied to the CT energy of the five dimers given in table 4, and the results are listed in the last three columns. From the difference between the corrected E_{CT} and E'_{CT}, it is clear that the total interaction energy calculated with the extended groups wavefunction does not differ appreciably from the value obtained with the HF-SCF calculation.

To explore the behavior of the BSSE in more detail, the interaction potentials of $HCOOH-NH_3$ and $HCOO^- - HNH_3^+$ have been obtained from both the NOGF and HF-SCF wavefunctions. The calculations were carried out with Roos−Siegbahn

(7s,3p) atomic basis sets which were contracted to double-zeta (DZ) molecular bases [61], a 4s basis contracted to DZ for hydrogen [46] and rigid fragment geometries [25]. The optimal energies and separations are given in table 5. It is seen that for both neutral pairs (NP) and charged pairs (CP), the BSSE corrected results are essentially identical. In addition, the differences between the corrected and

Table 5

Effect of BSSE on the interaction potential.

	NH_3HCOOH	
Ψ	R_{min} (Å)	E_{min} (kcal/mole)
2 grps	2.76	– 14.8
2 grps + BSSE	2.77	– 13.0
HF-SCF	2.71	– 16.5
HF-SCF + BSSE	2.78	– 13.1
	$NH_4^+OOCH^-$	
2 grps	2.50	– 134.4
2 grps + BSSE	2.51	– 129.0
HF-SCF	2.47	– 139.7
Hf-SCF + BSSE	2.51	– 131.4

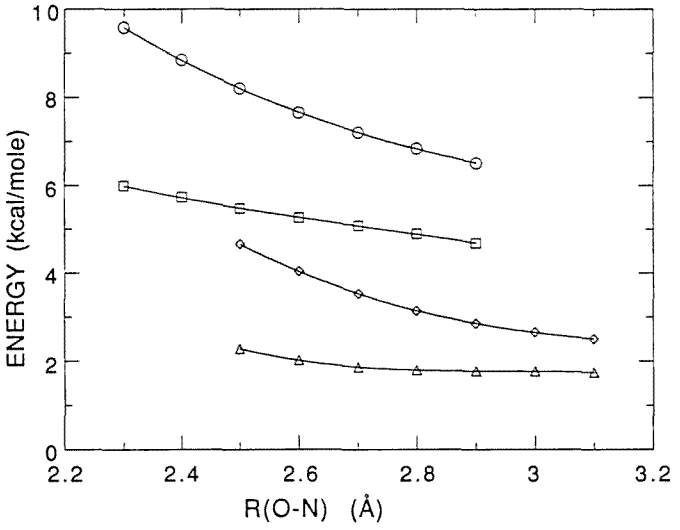

Fig. 2. Basis set superposition error as a function of interfragment separation of ammonia-formic acid. O SCF: $HCOO^-HNH_3^+$; □ 2 grp NOGF: $HCOO^-HNH_3^+$; ◇ SCF: $HCOOHNH_3$; Δ 2 grp NOGF: $HCOOHNH_3$.

uncorrected potentials are smaller when calculated using the NOGF approximation than when using the standard SCF method. Thus, for the former the difference in the optimal separation is only 0.01 Å, whereas the latter gives differences of 0.07 Å and 0.04 Å for the NP and CP, respectively. This behavior was already noted earlier in a comparison of the NOGF and HF-SCF interaction potentials of the water dimer [21]. The reason for the decreased effect of the BSSE on the NOGF interaction potential can be seen in fig. 2, where the BSSE correction has been plotted as a function of distance for both NP and CP. The BSSE effect is smaller, but in addition, the curves are much flatter so that they shift the potential curves somewhat on the energy axis but do not alter the slopes, and hence the minimum position is also not appreciably changed. In contrast, the BSSE correction curve calculated with the HF-SCF wavefunction has a larger slope and therefore distorts the potential more. Finally, it is worthwhile to note that the BSSE correction is easier to calculate in the NOGF approximation since $\Delta E'_{\mathrm{BSSE}}$ is obtained from a smaller HF-SCF problem than ΔE_{BSSE}.

3.4. MANY-BODY EFFECTS

Many-body effects which cannot be fully described by effective, additive pair potentials are of considerable importance in the study of condensed phases. Recent studies have shown that they can be significant in determining the relative stability of closely related configurations of solvation shells [62] and for the reliability of Monte Carlo or molecular dynamics simulations [63]. Thus, in a recent simulation [64] to calculate the dielectric constant of water using the MCY potential [65], it was suggested that the large error in the theoretical value was at least partially due to the lack of proper accounting of nonadditivity effects by this potential. Moreover, it was suggested that reparametrization alone would probably not be sufficient [64].

Although there is general agreement that these effects will ultimately have to be included in the potential functions used in computer simulations, at present their functional form and relative importance have not been extensively studied. In terms of the energy decomposition given above, the exchange, induction and charge transfer effects are all nonadditive [66]. Of these, only the induction can be described with the help of classical electrostatic theory, while both exchange and charge transfer are quantum effects, although the short range of the exchange interaction often leads to very small three- and higher-body contributions (see below). To study many-body effects, the interaction potential is decomposed in the form [67]

$$U(r_1, r_2, \ldots, r_n) = \sum_i U^{(1)}(r_i) + \sum_{i<j} U^{(2)}(r_i, r_j) + \ldots \tag{3.13}$$

and the interaction energy is now $\Delta E = U - \sum U^{(1)}$.

The NOGF approximation is particularly well suited for analyzing many-body effects. To effect the decomposition of U to, say, the m-mer level, one computes the NOGF wavefunction for m groups and subsequently all the l-mers ($l < m$) which

can be constructed from the m-mer. Since the geometry is kept frozen for this process, the two-electron integrals need to be calculated only once for the m-mer, and then for each l-mer the corresponding set of integrals can be extracted from the m-mer's list, thus making the decomposition fairly economical.

A trimer of formamide modelling main chain α helical H-bonding [23] was studied using a wavefunction of the form

$$\Psi = \mathcal{A}'[\Phi_i \Phi^e_{i+3} \Phi^e_{i+6}], \tag{3.14}$$

where the group function subscripts denote the peptide positions in the α helix which are H-bonded [68]. The calculations were carried out with minimum basis (MB) sets [69]. The results of the energy decomposition are summarized in table 6.

Table 6

Energy decomposition of nonadditivity effects[a].

	Formamide			Water			
	$-E$	$-E$	$-U^{(3)}$	$-E$	$-E$	$U^{(3)}$	$U^{(3+4)}$
	$i, i+3$	$i, i+3, i+6$		$(H_2O)_2$	$(H_2O)_3$		
C + EX	2.2	5.0	0.04	2.6	6.0	0.11	0.06
Pol	0.9	2.4	0.6	1.4	3.6	0.7	0.3
CT	1.7	3.6	0.2	2.1	4.7	0.4	0.1
ΔE	4.8	10.9	0.8	6.2	14.3	1.2	0.5
Polarization and reaction field effects							
Pol(i)	0.29	0.34	0.05				
Pol($i+3$)	0.51	1.16	0.35				
Pol($i+6$)		0.58	0.07				
Σ	0.81	2.07	0.47				
Pol	0.89	2.35	0.57				

[a] Energy in kcal/mole; see text for definitions of quantities.

The main three-body contribution comes from the induction and comprises about 25% of the total polarization energy, and the CT contribution to $U^{(3)}$ is about 8% of the total CT contribution. Note also that the small C + EX contribution is due to exchange interactions since the electrostatic component is pair additive.

The group product structure of the NOGF wavefunction allows for a further decomposition of the polarization (or charge transfer) effects into a primary and secondary contribution. The former corresponds to the polarization of a group in the field of the remaining unperturbed groups, whereas the latter is the group's response due to the polarization of its neighbors and is thus analogous to the

reaction field [70]. The primary effect for any group is calculated by solving the NOGF-SCF eqs. (2.31) for the group in the field of the other unperturbed groups. The wavefunction is

$$\Psi_2(R) = \mathcal{A}'[\Phi_1^0 \ldots \Phi_R \ldots \Phi_T^0], \tag{3.15}$$

from which $E_{\text{pol}}(R)$ can be calculated. Table 6 lists these quantities for the dimer and trimer of formamide, and the contribution to $U^{(3)}$. Not surprisingly, the $i+3$ fragment makes the largest contribution in the trimer and yields the largest three-body effect. Moreover, the secondary "reaction field" effects contribute an additional 10% to E_{pol} in both dimer and trimer, but about 20% to $U^{(3)}$.

The convergence behavior of the many-body contribution was studied in an ice-like chain of five water molecules [22] using 4-31G basis sets [52]. The results are also summarized in table 6. Overall, the behavior here is similar to the formamide case. $U^{(3)}$ consists of only nearest-neighbor three-body terms, whereas the remaining three- and four-body terms are summed together in the column $U^{(3+4)}$. The ordering of the contributions to $U^{(3)}$ is (in magnitude) Pol > CT $\gg$ C + EX, which is different than for $U^{(2)}$ where it usually is C + EX > CT > Pol. The total contribution to $U^{(3+4)}$ is about half again as much as $U^{(3)}$ and about half comes from the remaining three-body interactions and half from all the four-body interactions. From the results of this analysis, it is possible to extrapolate to infinite chain length and a value of -9.4 kcal/mole H-bond was obtained, which is to be compared with a value of -7.4 kcal/mole H-bond if only pair interactions are considered [22]. Thus, in the present model, higher-order effects enhance the interaction energy by about 20%, but it must be added that other systems have been studied where these effects are repulsive [71].

3.5. FURTHER APPROXIMATIONS FOR THE REGION Ib

Due to the nonvanishing overlaps between the fragments in regions Ia and Ib (fig. 1), all the intermolecular effects derived from the energy decomposition will, in principle, influence the way that the molecular fragments in region Ib modulate the interactions in region Ia. However, the Ib charge distributions are not directly involved in the interactions under consideration in systems represented by fig. 1, nor are they the targets of any chemical changes occurring in region Ia. Thus, it does not seem unreasonable to expect that these nearest neighbors of the active part of the system can be treated at a more approximate level than the charge distributions in region Ia.

Two features of the NOGF approximation have been used to formulate models where the NNF are treated more approximately than the AF. First is the effectiveness of the screening operator to keep the charge density of each group localized in its own proper subspace. This suggests that if bases of different quality are used for expanding the orbitals of the groups, the screening operator will prevent any distortion

in the wavefunction. Thus, the NNF can be expanded with smaller bases than the AF. Second, the structure of the orbital equations (2.31) allows each group to be optimized independently in the effective field of the other groups. It is therefore possible to predetermine the orbitals of some groups, e.g., the NNF, in a smaller subsystem and then transfer these orbitals to the system of interest, where they are held frozen, i.e., their orbitals are not modified by the iterative procedure. Finally, it can be assumed that in some cases it is not necessary to include all the interactions between NNF and AF to describe the modulating effect of the former. In these latter cases the NNF's groups are not extended but only the Coulombic, exchange and polarization interactions are incorporated. To show that different basis sets are used, the previous notation for the wavefunctions is modified to

$$\Psi = \mathcal{A}'[\Phi_1^A \Phi_2^B \ldots \Phi_T^K] \equiv [1{:}A, 2{:}B, \ldots, T{:}K], \tag{3.16}$$

where $A, B, \ldots$ refer to the groups' basis sets. Finally, the notation is further simplified as given by the r.h.s. of eq. (3.16).

To fix these ideas more firmly, consider the effect of using mixed basis sets to calculate the effect of hydration on the protonation energy (PE) of formate, ammonia, guanidine (GD) and imidazole (IMI) [25]. In this example, the water molecules are considered as NNF and two are H-bonded to each AF. Standard supermolecule calculations were carried out using the 4-31G basis [52] and Gauss80 [60]. A mixed basis was formed, where the acid and bases are described by a DZ basis constructed from (7s,3p) [61] atomic bases and a (4s) basis [46] for hydrogen, and an MB basis [69] for the waters. An example of the geometric arrangement of the waters around the AF is given in fig. 3 for the acid and ammonia for the neutral and ionized species. The geometries of the isolated fragments and complexes have been given elsewhere [25]. For the calculations discussed here, each AF–NNF cluster is treated as an isolated system, but their interactions will be considered below.

To account for all the interactions, extended groups have to be used for the PAs, which in the case of formate is the acid, but for the bases the waters are the PAs. Thus, for NH_3, NH_4^+, IMI, $IMIH^+$, GD and GDH^+, the wavefunction for the mixed basis is

$$\Psi = [\mathrm{AF}{:}\,\mathrm{DZ}, \mathrm{H_2O}{:}\,\mathrm{eMB}, \mathrm{H_2O}{:}\,\mathrm{eMB}], \tag{3.17a}$$

but for the acid, the wavefunction is

$$\Psi = [\mathrm{AF}{:}\,\mathrm{eDZ}, \mathrm{H_2O}{:}\,\mathrm{MB}, \mathrm{H_2O}{:}\,\mathrm{MB}]. \tag{3.17b}$$

In constructing the orbitals for the extended groups, care must be taken that the same level of approximation is used for all the basis functions. Thus, in eq. (3.17a) the proton's basis is included with the waters at the MB level, but in eq. (3.17b) the proton is described at the DZ level.

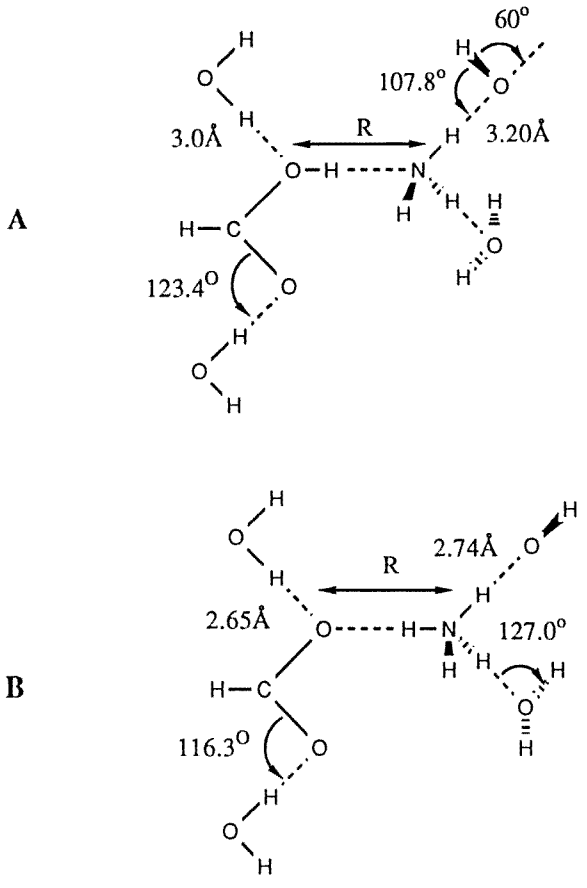

Fig. 3. Conformation and interfragment geometries of ammonia–formic acid complex. A: neutral pair; B: charged pair. For additional geometric details, see ref. [25].

First the PEs of the isolated species using the 4-31G or DZ basis sets were calculated with a one-group wavefunction, and subsequently the hydrated complexes were determined using the three-group wavefunctions of eqs. (3.17). Table 7 shows the shift in PE upon hydration of the isolated species as calculated with standard HF-SCF wavefunctions and the mixed basis, three-group wavefunction. The shifts differ by 1 kcal/mole or less, showing that the three-group wavefunction using the mixed basis set responds as effectively to hydration as the standard single-determinantal wavefunction.

To assess the other approximations, the subsystem $2(H_2O)HCOO^-$ and NH_4^+ are used to set up an interacting system where the formate and ammonium are in a double H-bonded configuration [25]. In this system, the waters are considered as NNF which modulate the H-bonding interaction between the formate and ammonium

Table 7

Shifts in protonation energies due to hydration[a].

Molecule	ΔPE[b] 4-31G	ΔPE[b] DZ/MB
$2(H_2O)HCOO^-$	28.3	27.2
$2(H_2O)NH_3$	-44.4	-44.3
$2(H_2O)$GD	-29.0	-28.6
$2(H_2O)$IMI	-25.3	-24.9

[a] Energies in kcal/mole.
[b] $\Delta PE = PE(\text{complex}) - PE(\text{isolated molecule})$.

ions. The interactions between the AFs are always fully represented, thus the basis from the two protons from ammonium which H-bond to the formate are included in the latter's orbital expansions. If the CT effect between the waters and formate is also included, the wavefunction has the form

$$\Psi = [NH_4^+: DZ, HCOO^-: eDZ, H_2O: A, H_2O: A], \tag{3.18a}$$

but if they are to be omitted, one has

$$\Psi = [NH_4^+: DZ, HCOO^-: DZ, H_2O: A, H_2O: A]. \tag{3.18b}$$

Note that in eq. (3.18a), "e" refers only to the CT interaction between water and formate. For this system, the interaction potential has been calculated for both the all-DZ basis (A = DZ) and the mixed basis (A = MB). The wavefunctions defined in eqs. (3.18a) and (3.18b) are denoted by "CT" and "Pol", respectively.

If the NNF's orbitals are to be kept frozen during the optimization of the AFs' orbitals, they must be determined from a suitable subsystem prior to starting the calculation. One possibility is to take them from the isolated H_2O wavefunction, and this case is designated by F. Alternatively, one can determine these orbitals from the subsystem $2(H_2O)HCOO^-$, excluding or including CT, and they are then designated by F′ and F″, respectively.

The interaction potentials for these different options are summarized in table 8. In these calculations the 4-group, fully optimized, CT wavefunction is used as the reference. This is fully justified from the discussions of previous sections and results reported elsewhere [21–25]. It is clear from table 8 that the DZ/DZ and DZ/MB CT; CT; F′; and CT, F″ wavefunctions all give essentially the same results. However, for locating the minimum, one can first use the Pol, F′ wavefunction and subsequently use the CF, F′ wavefunction to calculate the interaction energy and final value of R_{min}. The reduction in computing time realized by these approximations lies between about 25% and 75% of the full CT calculation, depending upon which wavefunction is being used. The HF-SFC calculation for this system requires about

Table 8

Minimum distances and interaction energies.

	DZ/DZ		DZ/MB	
Ψ	R_{min} [a]	$\Delta\Delta E_{min}$ [b]	R_{min} [a]	$\Delta\Delta E_{min}$ [b]
CT	2.867	0.0	2.859	-1.0
CT,F′	2.863	-0.1	2.860	-0.8
CT,F″	2.864	0.3	2.861	-0.5
CT,F	2.854	-3.7	2.854	-3.4
Pol	2.845	-4.6	2.843	-5.5
Pol,F′	2.846	-4.7	2.844	-5.5
Pol,F	2.837	-8.5	2.837	-8.2

[a] R_{min} is the C–N distance at the minimum in Å; see ref. [25] for geometries.

[b] $\Delta\Delta E_{min}$ is the energy difference relative to the interaction energy of CT in kcal/mole.

60–70% of the CT wavefunction in the current version of the program, which has not been fully optimized. Moreover, for the reasons discussed in the previous section, the NOGF approximation will become increasingly economial relative to standard methods with increasing system size.

3.6. EFFECTS OF ENVIRONMENT ON ION PAIR FORMATION AND PROTON TRANSFER

Ion pair formation is of fundamental importance in controlling the structure and function of enzymes. Such pairs contribute significantly to protein stability [73] and the proton transfer reactions between these pairs are involved in innumerable enzymatic reactions. Both experimental [74–76] and theoretical studies [77,78] have suggested that these types of interactions are subtly modulated by the nearest environment, so it should not be surprising that even the simplest models are rich in insight. The question to be addressed here is how the interaction potential of an interacting pair in the charged and uncharged states is influenced by hydrogen bonding of the pair's fragments to neighboring molecules, and which components of the interaction are the main source of the changes.

The model consists of a formic acid interacting with ammonia. Each fragment is H-bonded to water molecules, as shown in fig. 3. Calculations were carried out for the CP (fig. 3A) and the NP (fig. 3B), and four systems were considered, i.e., the isolated pairs, the pairs with two waters bound to either the acid or the base, and the pairs with four bound waters. The quantity of interest is the energy change of the reaction

$$AH-B = A^{-}-BH^{+}, \tag{3.19}$$

where

$$\Delta E = E(A^- - BH^+) - E(AH - B), \tag{3.20}$$

which is just the energy change obtained from changing the neutral pair to a charged pair. It is convenient to consider the reaction (3.19) as part of a closed cycle

$$\begin{array}{ccc} & \overset{\Delta E}{} & \\ AH-B & = & A^- - HB^+ \\ \Delta E_{AB} \quad || & & || \quad \Delta E_{A^-B^+} \\ AH + B & = & A^- + BH^+ \\ & \underset{\Delta PE}{} & \end{array} \tag{3.21}$$

From eq. (3.21), it is seen that ΔE can also be expressed as

$$\Delta E = \Delta E_{A^-B^+} + \Delta PE - \Delta E_{AB} \tag{3.20'}$$

$$= \Delta E_{A^-B^+}(\text{net}) - \Delta E_{AB}. \tag{3.20''}$$

The first and third terms on the r.h.s. of eq. (3.20′) are just the stabilization energies of the CP and NP, while ΔPE is the difference in the protonation energies between the two fragments, i.e. $PE(BH^+) - PE(AH)$, and can be regarded as the work required to charge the two fragments at infinite separation. In eq. (3.20″), the CP's interaction energy and ΔPE have been combined to give the net stabilization energy of the CP. This is convenient because $\Delta E_{A^-B^+}(\text{net})$ and ΔE_{AB} now refer to the same value of zero on an energy scale.

The reaction cycle (3.21) is written for the isolated pair. One can also consider the pair embedded in an environment S, for which the reaction cycle takes the form

$$\begin{array}{ccc} & \overset{\Delta E^S}{} & \\ S(AH-B) & = & S(A^- - HB^+) \\ \Delta E^S_{AB} \quad || & & || \quad \Delta E^S_{A^-B^+} \\ SAH + SB & = & SA^- + SBH^+ \\ & \underset{\Delta PE^S}{} & \end{array} \tag{3.22}$$

and

$$\Delta E^S = \Delta E^S_{A^-B^+} + \Delta PE^S - \Delta E^S_{AB} \tag{3.23'}$$

$$= \Delta E^S_{A^-B^+}(\text{net}) - \Delta E^S_{AB}. \tag{3.23''}$$

Thus, from the reaction cycles (3.21) and (3.22) it is possible to express the energy of ion pair formation in terms of the pair's stabilization energy and the self energy as expressed by ΔPE.

In the calculations, the formic acid and ammonia are the AFs of region Ia (fig. 1) and the waters are NNF belonging to region Ib and designated by "S" in

the notation of eqs. (3.22) and (3.23), 2-, 4-, or 6-group wavefunctions are constructed, depending on the number of water molecules included. The wavefunction structure is similar to that described above (eqs. (3.16) and (3.17)) with the water orbitals expanded at the MB [69] level and the AF with a DZ [61] basis. In all cases, the NNF orbitals are frozen, and the orbitals of the waters H-bonded to the acid were determined from a Pol-type wavefunction for the formate–$2(H_2O)$ fragment, but for reasons discussed elsewhere [25], the orbitals of the waters H-bonded to ammonia were obtained from the wavefunction of the fragment ammonia–$2(H_2O)$ including CT. The geometries of the fragments are as in the previous section and are kept fixed while the formate–ammonia distance is varied (R in fig. 3), and finally each NNF–AF fragment is moved as a rigid body.

Fig. 4. Interaction potentials for hydrated ammonia–formic acid complex. Ionized pair, solid curves; neutral pair, dashed curves. ○ AB; □ 2SAB; ◇ AB2S; △ 2SAB2S; S = H_2O, A = HCOOH($HCOO^-$); B = NH_3(NH_4^+).

The potential curves of the CP and NP in the different degrees of hydration are shown in fig. 4. The water molecules affect both NP and CP in the same way in that the potential curves are lowered with increasing hydration. However, the effect is much stronger for the CP than the NP. This results in a large change in the relative energies of the CP and NP, which is about 20 kcal/mole favoring the isolated pair, but has been reduced to about 3 kcal/mole for the pair hydrated with four waters. Similar results are found for two other models of ion pair interactions: For formic acid–histidine the isolated CP lies 17 kcal/mole above the NP, but for the pair hydrated with four waters the former is 3 kcal/mole below the latter [79]. The formic–guanidine pair behaves in the same way, but for this pair the CP lies

below the NP even for the isolated case [79]. Thus, hydration changes the relative energy from −4 to −20 kcal/mole.

The minimum value of R as well as the energy quantities defined by the reaction cycles (3.21) and (3.22) are given in table 9. It is of interest to note that the minimum separation decreases in the NP, but increases in the CP with increasing hydration. As already seen from fig. 4, ΔE_{AB} decreases by about 7.5 kcal/mole on

Table 9

Interaction potential for hydrated formate–ammonia.

System[a]	NP		CP				
	R_m	ΔE_{AB}	R_m	$\Delta E_{A^-B^+}$	ΔPE	$\Delta E_{A^-B^+}$(net)	ΔE[b]
AB	2.76	−14.7	2.49	−134.4	141.6	7.2	21.9
2SAB	2.72	−17.7	2.53	−115.4	117.0	1.6	19.3
AB2S	2.73	−18.3	2.58	−107.1	98.0	−9.1	9.2
2SAB2S	2.68	−22.3	2.62	−92.4	73.4	−19.0	3.3

[a] A = HCOOH; B = NH_3; S = H_2O; energies in kcal/mole.
[b] $\Delta E = \Delta E_{A^-B^+}(\text{net}) - \Delta E_{AB}$.

hydration with four H_2O. However, $\Delta E_{A^-B^+}$ increases with hydration. Thus, the H-bonded waters destabilize the CP with respect to the hydrated, isolated charged fragments. The shift is about 45 kcal/mole, but opposed to this is the change in ΔPE, which decreases by about 70 kcal/mole. The net effect, therefore, is that hydration stabilizes the CP by about 26 kcal/mole, which is about 3.5 times greater than the stabilizing effect on the NP. Moreover, this effect is due to the presence of only four water molecules in the immediate neighborhood of the interacting pair. The effect of bulk solvent has not been included in the calculation.

The above analysis has been carried out by considering the effects of H-bonded interactions on the pairs' binding energies and the self energies of the charged fragments. The results clearly indicate that the latter quantity determines the relative shifts in stability of the CP and NP. This is not unexpected, but what is perhaps surprising is the size of the shift caused by only two waters H-bonded to each fragment. There is, however, another point of view which suggests that the relevant quantity is the change in energy resulting from the transfer of the pair from one solvent to another [80,81]. In the present case, this "transfer" is from the gas phase (vacuum) to the hydrated phase (pair interacting with H-bonded waters). This process can also be represented by an interaction cycle, i.e.,

$$\begin{array}{ccc} & \Delta E^S & \\ S(AH-B) & = & S(A^--HB^+) \\ \Delta S^S_{AB} \quad || & & || \quad \Delta S^S_{A^-B^+} \\ S + AH-B & = & S + A^- - BH^+ \\ & \Delta E & \end{array} \tag{3.24}$$

and ΔE^S is calculated from

$$\Delta E^S = \Delta E + \Delta S_{A^-B^+} - \Delta S_{AB} . \tag{3.25}$$

The quantities $\Delta S_{A^-B^+}$ and ΔS_{AB} have also been calculated and are summarized in table 10. They correspond to the transfer described by the reaction cycle (3.24) and the values of ΔS_{AB} and $\Delta S_{A^-B^+}$ show that the interaction of the waters with the AFs stabilizes both the CP and the NP, but the former more than the latter.

Table 10

Effect of "solvation" energy on stability[a].

	ΔE^S	ΔE	ΔS_{AB}	$\Delta S_{A^-B^+}$
2S + AB ↔ 2SAB	19.3	22.0	- 13.7	- 16.4
2S + AB ↔ AB2S	9.2	22.0	- 8.9	- 21.7
4S + AB ↔ 2SAB2S	3.3	22.0	- 23.4	- 42.1

[a] Energies in kcal/mole; A = HCOOH, B = NH_3; S = H_2O; quantities defined in eq. (3.24).

The two viewpoints represented by reaction cycles (3.21) and (3.22) on the one hand, and (3.25) on the other, are complementary. Both exhibit the very large modulating effects originating in the interactions of AF with the nearest neighbors but emphasize different aspects. The former shows the key role of the self energy in stabilizing ion pairs, while the latter seems to be more instructive when comparing the transfer of an interacting pair from one environment to another, such as water to protein. In any case, the discussion and results of the last two sections indicate that with the NOGF approximation, it should be possible to give an adequate description of these types of interactions using models where both the active part of the system and its nearest neighbors are considered at the quantum mechanical level.

The analysis developed in the previous section can also be used to study the effect of environmental hydrogen bonding on proton transfer (PT) potentials. A number of studies [82–85] have demonstrated that environmental effects can have a strong influence on the shape of proton transfer potentials, which is of particular importance in the analysis of enzymatic reactions. Models of the type used here are helpful in exhibiting the individual effects and in providing some insight into their relative importance.

The model, basis sets and group structure of the wavefunction are the same as above (fig. 3) and the effects of two waters H-bonded to the acid and/or the base are considered. The PT potentials have been calculated with an N–O distance of 2.9 Å, and the geometries of the acid, base and waters were not optimized at each point where the potential was calculated. Instead, two calculations are carried out, one using the NP geometry (fig. 3A) and the other using the CP geometry (fig. 3B).

The structure yielding the lowest energy at a given point is then used to approximate the potential at that point. This technique was shown to give quite reasonable results, and, of course, saves considerable computing time [86].

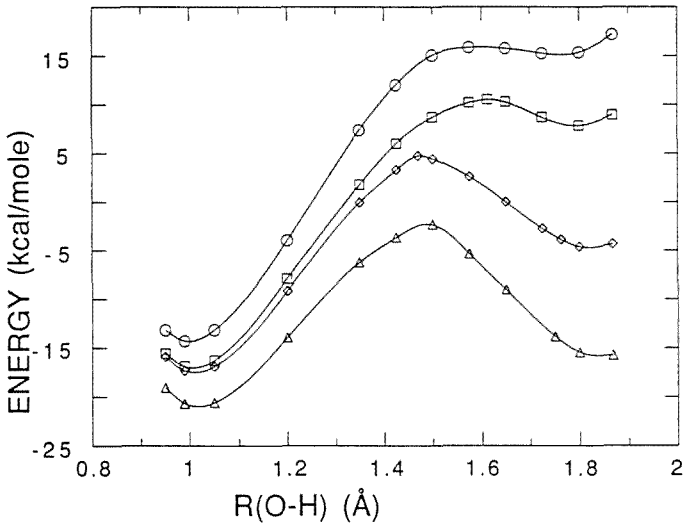

Fig. 5. Proton transfer potentials for ammonia–formic acid; symbols as in fig. 4.

Table 11

Minima and barrier maximum for proton transfer.

	AH–B[a]		A–H–B[a]		A^-–HB^+[a]	
System	R_{min}[b]	$\Delta E(NP)_{min}$[c]	R_{max}[b]	ΔE_{max}[d]	R_{min}[b]	$\Delta E(CP)_{min}$[c]
AB	1.00	30.2	1.59	29.5	1.76	0.7
2SAB	1.01	27.6	1.63	24.8	1.80	2.8
AB2S	1.01	22.2	1.47	12.7	1.83	9.5
2SAB2S	1.02	18.7	1.49	5.0	1.84	13.7

[a] A = HCOOH; B = NH_3; S = H_2O; energies in kcal/mole.
[b] R(O–H) in Å.
[c] $\Delta E(i)_{min} = E_{max} - E(i)_{min}$; $\Delta E_{max} = E(CP)_{min} - E(NP)_{min}$.

The PT potentials for the four systems are plotted in fig. 5 and the values of the minima and barrier heights are given in table 11. The energies are calculated as defined in the reaction cycles (3.21) and (3.22). Figure 5 shows that the curves move downward with increasing hydration, but as for the interaction potentials, the effect is much stronger on the CP side of the reaction than on the NP side. The O–H minimum distance increases slightly for the NP, but the H–N optimal

distance decreases by nearly 0.1 Å in the CP with four water molecules. Furthermore, the NP barrier decreases by about 10 kcal/mole, while the CP barrier, which is practically zero for the isolated pair, increases to nearly 14 kcal/mole when the pair is H-bonded to four waters. The position of the barrier's maximum shifts away from the AF which is hydrated and is substantially greater for hydration of the ammonia.

Using the energy decomposition scheme developed for the NOGF approximation and eqs. (3.20) and (3.21), the energetics of the PT potential at both minimum values have been decomposed and the results are listed in table 12. As for the

Table 12

Proton transfer energy decomposition[a].

	ES	ΔPE	ES_{net}	EX	CT + Pol	ΔE	ΔE_{net}
A^-–HB^+	– 116.4	144.2	27.8	8.1	– 20.8	– 129.1	15.1
SA^-–HB^+	– 113.5	119.7	6.2	35.0	– 33.6	– 112.1	7.6
A^-–HB^+S	– 111.8	100.9	– 10.9	29.5	– 23.4	– 105.7	– 4.8
SA^-–HB^+S	– 110.4	76.4	– 34.0	56.4	– 37.9	– 91.9	– 15.5
AH–B	– 17.3			9.6	– 6.8		– 14.5
SAH–B	– 19.3			15.2	– 13.1		– 17.2
AH–BS	– 20.8			14.8	– 11.7		– 17.7
SAH–BS	– 23.1			20.4	– 18.4		– 21.1

[a] Energy in kcal/mole; ES = electrostatic energy; EX = exchange energy; CT + Pol = charge transfer + polarization; EX, CT + Pol is calculated for all interactions; S = $2H_2O$.

interaction potentials, hydration destabilizes the CP side of the PT relative to the isolated, charged fragments. This effect is primarily due to the large contributions to the EX energy from each fragment, while the ES increases only slightly. Again, ΔPE determines the response of the net interaction energy to the presence of the NNF, although the contribution of CT + Pol is also substantial and favors hydration. On the NP side of the PT, the combined effect of the ES and CT + Pol is more stabilizing than the EX contributions destabilizing the interaction, which results in the overall effect favoring the addition of H-bonded waters to the AF.

The effect of four waters H-bonded to the formate–ammonia pair results in the creation of a substantial barrier for shifting the proton from the CP side to the NP side. It is clear from these results that changes in H-bonding patterns between the AFs and NNF can provoke very large changes in the PT potential which even seem to include the possibility of changing a single well to a double well potential. Since it has also been shown that changes in geometry affect the PT potential [87], it appears that systems like enzymes possess a number of mechanisms whereby proton transfer reactions can be initiated and controlled.

4. Conclusions

The self-consistent, nonorthogonal group function approximation is an ab initio approach for calculating the electronic structure of large molecular aggregates. The formulation of the method as presented here is completely general, and thus applicable to any closed shell system. Since the orbital equations are derived by requiring that suitably defined group energy functionals are stationary rather than the total energy, the NOGF wavefunction is an approximation to the restricted HF-SCF wavefunction. However, the applications presented here have shown that for hydrogen-bonded systems, the results are negligibly different from the standard SCF results. Indeed, due to the partial accounting of the BSSE inherent in the NOGF wavefunction, calculated interaction energies (and other properties) are less distorted than the corresponding quantities obtained from the HF-SCF wavefunction.

As discussed in the formulation, the structure of the orbital equations in the NOGF approximation implies a third power dependence of computational effort with system size. However, by using mixed basis sets and freezing groups it is further reduced, and for the hydrated ion pairs studied here lies between a linear and quadratic dependence [25]. It is clear, therefore, that NOGF theory would provide a practical approach for studying the effects of macromolecular environment on the electronic structure of active groups in enzymes. In addition, it may be feasible to implement the method in molecular dynamics calculations to calculate changes in the interaction potential "on the fly".

For the future, a number of further developments are essential for the general applicability of the method. Some of these are further optimization of the current program and adaption to vector and parallel processing, extension to open shell systems, and incorporation of environmental effects from regions II and III in fig. 1. Some of these are currently being implemented, and their completion will result in a considerable extension in the types of problems which can be studied at the ab initio quantum chemical level.

Acknowledgements

The author gratefully acknowledges the partial support of NIH Grant GM-41373 and the Swiss National Science Foundation Grants 31-8840.86 and 31-26261.89. I would also like to thank the University of Basel Computer Center for their support and generous grants of computing time.

References

[1] J. Simons, J. Phys. Chem. 95(1991)1017.
[2] I. Flemming, *Frontier Orbitals and Organic Chemical Reactions* (Wiley, London, 1976).
[3] R.J. Bartlett, J. Phys. Chem. 93(1989)1697.
[4] R. Ahlrichs and P. Scharf, *Ab Initio Methods in Quantum Chemistry*, Vol. 1, ed. K.P. Lawley (Wiley, 1987), pp. 501–537.

[5] B.O. Roos, ibid., Vol. 2, pp. 399–446.
[6] H.-J. Werner, ibid., pp. 1–62.
[7] W.J. Hehre, L. Radom, P. von Schleyer and J.A. Pople, *Ab Initio Molecular Orbital Theory* (Wiley, New York, 1986).
[8] E. Clementi, G. Corongiu and S. Chakravorty, in: *Modern Techniques in Computational Chemistry*, ed. E. Clementi (ESCOM, Leiden, 1990), pp. 343–434.
[9] A. Warshel, Nature 330(1987)15.
[10] J. Warwicker and H.C. Watson, J. Mol. Biol. 157(1982)671.
[11] E.L. Mehler and G. Eichele, Biochem. 23(1984)3887.
[12] A. Warshel and M. Levitt, J. Mol. Biol. 103(1976)227.
[13] M.L.J. Drummond, Progr. Biophys. Mol. Biol. 47(1986)1.
[14] O. Tapia, in: *Molecular Interactions*, Vol. 3, ed. H. Ratajczak and W.J. Orville-Thomas (Wiley, 1982), pp. 47–117.
[15] G. Karlström, J. Phys. Chem. 92(1988)1315, 1318.
[16] B.T. Thole and P.T. van Duijnen, Theor. Chim. Acta 55(1981)307.
[17] R. Ahlrichs, Theor. Chim. Acta 33(1974)157.
[18] Y. Dycmons, ibid. 28(1973)307.
[19] S. Wilson, *Electron Correlation in Molecules* (Clarendon Press, Oxford, 1984), pp. 208–220, and references therein.
[20] E.L. Mehler, J. Chem. Phys. 67(1977)2728 (part I).
[21] Ibid. 74(1981)6298 (part II).
[22] M.P. Fülscher and E.L. Mehler, Int. J. Quant. Chem. 29(1986)627.
[23] E.L. Mehler, J. Amer. Chem. Soc. 102(1980)4051.
[24] M.P. Fülscher and E.L. Mehler, J. Mol. Struct. (THEOCHEM) 165(1988)319.
[25] M.P. Fülscher and E.L. Mehler, J. Comp. Chem. 12(1991)811.
[26] J.M. Norbeck and R. McWeeny, Chem. Phys. Lett. 34(1975)206.
[27] J.M. Parks and R.G. Parr, J. Chem. Phys. 28(1958)335.
[28] M. Klessinger and R. McWeeney, J. Chem. Phys. 42(1965)3343.
[29] R. McWeeny, *Methods in Molecular Quantum Chemistry* (Academic Press, London, 1989), chap. 14.
[30] W.H. Adams, J. Chem. Phys. 34(1961)89.
[31] Ibid. 37(1962)2009.
[32] T.L. Gilbert, Phys. Rev. A6(1972)580.
[33] T.L. Gilbert, J. Chem. Phys. 60(1974)3835.
[34] O. Matsuoka, J. Chem. Phys. 66(1977)1245.
[35] K.R. Sundberg, J. Bicerano and W.N. Lipscomb, J. Chem. Phys. 71(1979)1515.
[36] H. Stoll and H. Preuss, Theor. Chim. Acta 46(1977)11.
[37] H. Stoll, G. Wagenblast and H. Preuss, ibid. 49(1978)67.
[38] P.O. Löwdin, Phys. Rev. 139(1965)357.
[39] A. Mazziotti, R.G. Parr and G. Simons, J. Chem. Phys. 59(1973)939.
[40] S. Huzinaga and A.A. Cantu, J. Chem. Phys. 55(1971)5543.
[41] A.B. Kunz, Phys. B6(1973)247.
[42] H. Schlosser, Chem. Phys. Lett. 23(1973)545.
[43] T.A. Koopmans, Physica 1(1933)104.
[44] E.L. Mehler, Int. J. Quant. Chem. S12(1978)407.
[45] S. Huzinaga, J. Chem. Phys. 42(1965)1293.
[46] T.H. Dunning, J. Chem. Phys. 53(1970)2823.
[47] D.E. Mann, P.A. Thrush, D.R. Lide, J.J. Ball and N. Acquida, J. Chem. Phys. 34(1961)420.
[48] K. Kitaura and K. Morokuma, Int. J. Quant. Chem. 10(1976)325.
[49] M. Dreyfus and A. Pullman, Theor. Chim. Acta 19(1970)201.

[50] P.A. Kollman and L.C. Allen, J. Chem. Phys. 52(1970)5085.
[51] K. Morokuma, J. Chem. Phys. 55(1971)1236.
[52] W.J. Hehre, R.F. Stewart and J.A. Pople, J. Chem. Phys. 51(1969)2657.
[53] P. Kollman, J. Amer. Chem. Soc. 99(1977)4875.
[54] H. Umeyama and K. Morokuma, ibid. 99(1977)1316.
[55] Z. Latajka and S. Scheiner, J. Mol. Struct. (THEOCHEM) 199(1989)9.
[56] J.R. Collins and G.A. Gallup, Chem. Phys. Lett. 123(1986)56.
[57] A. Vibol and I. Mayer, J. Mol. Struct. (THEOCHEM) 170(1988)9.
[58] S.F. Boys and F. Berardi, Mol. Phys. 19(1970)558.
[59] M. Gutowski, F.B. van Duineveldt, G. Chalasinski and L. Piela, Mol. Phys. 61(1987)2331.
[60] D.W. Schwenke and D.G. Truhlar, J. Chem. Phys. 82(1985)2418.
[61] B. Roos and P. Siegbahn, Theor. Chim. Acta 17(1970)209.
[62] A. Rahmouni, E. Kochanski, R. Wiest, P.E.S. Wormer and J. Langlet, J. Chem. Phys. 93(1990)6648.
[63] H. Saint-Martin, C. Medina-Llanos and I. Ortega-Blake, J. Chem. Phys. 93(1990)6448.
[64] M. Neumann, J. Chem. Phys. 82(1985)5663.
[65] O. Matsuoka, E. Clementi and M. Yoshimine, J. Chem. Phys. 64(1976)1351.
[66] A.D. Buckingham, in: *Modelling Molecular Structures and Properties*, ed. J.L. Rivail (Elsevier, Amsterdam, 1990), pp. 17–26.
[67] D. Hankins, J.W. Moskowitz and F.H. Stillinger, J. Chem. Phys. 53(1970)4544.
[68] J.S. Richardson and D.C. Richardson, in: *Prediction of Protein Structure and the Principles of Protein Conformation*, ed. G.D. Fasman (Plenum, New York, 1989), pp. 1–98.
[69] P. Graf and E.L. Mehler, Int . J. Quant. Chem. QBS8(1981)49.
[70] L. Onsager, J. Amer. Chem. Soc. 58(1936)1486.
[71] E. Kochanski, Chem. Phys. Lett. 133(1987)143.
[72] W.J. Hehre, W.A. Lathan, R. Ditchfield, M.D. Newton and J.A. Pople, Quantum Chemistry Program Exchange, Program No. 236, University of Indiana, Bloomington, Indiana.
[73] A.R. Fersht, J.-P. Shi, J. Krull-Jones, D.M. Lowe, A.J. Wilkinson, D.M. Blow, P. Brick, P. Carter, M.M.Y. Waye and G. Winter, Nature 314(1985)235.
[74] A.J. Russel and A.R. Fersht, Nature 328(1987)496.
[75] S. Linse, C. Johanssen, P. Brodin, T. Grundström, T. Drakenberg and S. Forsen, Biochem. 30(1991)154.
[76] R.L. Cutler, A.M. Davies, S. Creighton, A. Warshel, G.R. Moore, M. Smith and A.G. Mauk, Biochem. 28(1989)3188.
[77] G.N.J. Port and A. Pullman, Int. J. Quant. Chem. S1(1974)21.
[78] F. Sussman and H. Weinstein, Proc. Nat. Acad. Sci. USA 86(1989)7880.
[79] M. Fuelscher, Development and application of the nonorthogonal group function approximation: Program development and calculations on water polymers, ion pairs and stabilization of functional groups in proteins, Ph.D. Thesis, University of Basel, Basel, Switzerland (1988).
[80] A. Warshel, Proc. Nat. Acad. Sci. USA 81(1984)444.
[81] A. Warshel and S.T.Q. Russel, Rev. Biophys. 17(1984)671.
[82] M. Hodoscek, D. Kocjan and T. Solmajer, Croat. Chem. Acta 57(1984)65.
[83] S. Nakagawa and H. Umeyama, J. Theor. Biol. 96(1982)473.
[84] B. Borstnik, D. Janezic and D. Hadzi, J. Mol. Struct. 138(1986)341.
[85] J.P. Dijkman, R. Osman and H. Weinstein, Int. J. Quant. Chem. 35(1989)241.
[86] S. Topiol, G. Mercier, R. Osman and H. Weinstein, J. Comp. Chem. 6(1985)581.
[87] S. Scheiner and E.A. Hillenbrand, Proc. Nat. Acad. Sci. USA 82(1986)2741.